Impact of Nanoparticle Characteristics on Heat Transfer Enhancement for Industrial Cooling Applications: A Comparative Study of Thermal Conductivity Models

Gousia Begum

Department of UG and PG Studies in Mathematics, Government Degree (Autonomous) College, Kalaburagi, Karnataka, INDIA

Email: gousia_phd@yahoo.com

Abstract:

In the extrusion of polymer sheets cooling the surfaces quickly and uniformly is one the most critical activity. Conventional methods of cooling using chill rolls can be improved by embedding nanofluids. This current article is aimed at analysing the heat transport in carbon nanotubes-based nanofluid by two advanced thermal conductivity models namely, the Yamada–Ota and Xue models. Among the most significant physical properties in the polymer extrusion and stretching sheet cooling process is the thermal conductivity, which defines the rate at which heat can be removed from the hot polymer sheet during cooling. This is crucial for controlling the solidification, thickness, and mechanical properties of the final film. The mathematical model is framed according to boundary layer approximation theory for momentum and energy equations and solved by MATLAB solver bvp4c.The study investigates the effects nanoparticle volume fraction, magnetic field strength, wall thickness variation, power-law index, and thermal relaxation time on momentum and energy profiles, with results presented graphically. The novel outcomes of this study shows that the Yamada–Ota model demonstrates 30.60% higher heat transfer rate compared to the Xue model for nanoparticle volume fraction $\phi = 0.03$ and $m = 1.5$.

Key words: Hybrid nanofluid, variable thickness surface, MATLAB, numerical analysis.

1. Introduction.

Recent advances in the field on Nanotechnology fascinated many researchers to investigate more advanced nanofluids. The proficiency of the nanofluids in the enhancement of Heat transfer and Thermal conductivity by adding Nanoparticles like copper, alumina, gold, silver to the base fluids such as ethylene glycol, water have many applications in Biomedicine, nuclear reactors, food Industries, chemical Industry, automobiles, electronics etc. Xuan and Li [1] studied enhancement of heat transfer of nanofluids in tube by suspending solid nanoparticles. A comparative study of mass and heat transfer in non-Newtonian fluids over a permeable stretching sheet is coated by Sandeep et al. [2]. Raju et al. [3] theoretically investigated mass and heat transfer of nanofluids over a cone considering the parameters magnetic effect, non-uniform heat source/sink and concluded that heat transfer rate is more in Maxwell and oldroyd -B nanofluids compared to Jeffrey nanofluid. Qureshi [4] studied radiative heat and mass transfer MHD nanofluid flow in the presence spherical Au-metallic nanoparticles. Sugunamma et al. [5] reported 3-D motion of heat transfer in two different ferro liquids. Reddy et al. [5] explored their study on Casson fluid suspended with Fe_3O_4 nanoparticles over an upper surface of paraboloid of revolution. Stagnation point flow of SiO_2-Al_2O_3 hybrid nanofluid for mixed convection parameter is investigated and dual solutions is obtained by [6]. Various applications of nanoparticles is explored by Khan et al. [7], and Boundary layer flow of nanofluid with magnetic effect.

Magnetohydrodynamic (MHD) effect has received a lot of attention by many authors in recent years due to its wide applications in the cooling process of a nuclear reactor, power generator, control of chemical waste and pollutants dissemination, and metallurgical applications. The entropy analysis of Boundary layer nanofluid flow with MHD effect over porous shrinking sheet is investigated by Rashid et al. [8]. The effect of hybrid nanofluid flow with MHD and Radiation past a shrinking sheet were proposed by Waini et al [9]. Ramana reddy et al [10] studied the impact of 3D MHD flow of ferrofluids, methanol & kerosene over a stretching a sheet considering nonlinear radiation and concluded that sundry physical quantities viscosity and nonlinear radiation parameters affects the flow. A similar study carried out by Punit Gowda et al [11]. They explored that a 2D ferromagnetic fluid flow over a stretching sheet with the magnetic dipole effect.

Marangoni convection is characterized as interface dissipative flow. Marangoni convection is produced due to variation in surface tension gradients, Recently Magneto-Marangoni convection boundary layer flow has attracted many researchers for its numerous applications in material science, chemical engineering, food industry, welding, thin liquid films etc. Marangoni convection phenomenon is widely used in art work. Vishnu Ganesha et al [12] numerically investigated the behavior Marangoni boundary layer flow of γ-Al_2O_3 nanoparticles suspended in ethylene glycol and water base fluids in the presence of magnetic field and nonlinear thermal radiation. P. Dadheech et al. [13] investigated the effect of Marangoni convection of gamma-alumina oxide nanofluid past porous stretching sheet in the presence of thermal radiation and magnetic field. Y. Lin et al [14] investigated Marangoni boundary layer flow of Cu-H_2O nanofluid with exponential temperature and radiation effect over geometric shapes and concluded that sphere shaped nanoparticle with lesser thermal conductivity has better heat transfer enhancement compared to other shaped nanoparticles. Hayat et al. [15] addressed the impact of carbon-water nanoparticles with thermal radiation effect on Marangoni convection with boundary layer flow. A similar study of Marongoni convection is carried out by many researchers considering different circumstances see refs [16]–[26]. The flow past a porous medium has significant applications in the field of material processing, geothermal energy, drying processes, fuel cell machineries, oil recovery, medical sciences, earth sciences and various industries. S. Mukhopadhay et al.[27] studied the effects of thermal radiation and variable viscosity of convective boundary layer flow past porous stretching sheet. K.Khanafer and K.Vafai [28] presented their review on nanofluids applications in porous medium. Dadeech et al. [29] investigated the Marangoni convective heat transfer effect of hybrid nanofluid flow of Copper Oxide-Silver nanoparticles with base fluid ethanol glycol passed through a porous stretching sheet.

Prandtl number is a dimensionless number, the ratio of momentum diffusivity to thermal diffusivity. Vishnu Ganesh et al [30] presented a numerical study of thermal transport characteristics of γ-Al_2O_3 nanofluids over a Riga plate and analyzed the boundary layer flow and viscosity using an effective Pr number model. A similar study over a channel is conducted by Saba et al [31]. A similar effective Pr number models for γ-Al_2O_3 / H_2O. and γ-Al_2O_3 / $C_2H_6O_2$ nanofluids is analysed by Rashidi et al [32], Gul et al [33] experimentally studied the the phenomena of spray distribution on stretching cylinder using γ-Al_2O_3 , Cu- H_2O based nanofluids. The optimal scheme model resulted the impact of effective Pr number. A Zaib et al [34] explored the influence of effective Pr number on mixed convective micropolar flow of gamma alumina oxide-water nanofluid driven from wedge. Numerical investigation of effective Pr number of gamma alumina oxide nanoparticles with magneto hydrodynamic effect of boundary layer flow over the melting stretching sheet was put forth by N Ganesh et al [35]. Qayyum & Sumaira [36] illustrated the effects of MHD & Marangoni convection over a hybrid nanofluid suspending copper nanoparticles in water and ethylene glycol base fluids. To the best of author knowledge, no investigation is reported on variable thickness stretching sheet with Yamada-Ota and Xue model utilising nanofluid using non-Fourier heat flux model.

2. Mathematical formulation.

Let us consider boundary layer flow in two-dimensional coordinate configuration in which variable thickness sheet is considered in x axis direction and y axis is taken perpendicular to flow direction. Detailed configuration is shown in figure 1.The following assumptions are used in this mathematical modelling.

Slendering surface moving velocity is considered as $u_w(x) = A_0(x + b)^m$ where A_0 and b are constants. The thickness of stretching sheet decreases in x axis direction and it is written in the form $y(x) = A_1(x + b)^{\frac{1-m}{2}}$ where A_1 stretching constant. Under the above-mentioned assumption, the boundary layer equations can be expressed in Cartesian coordinate system as:

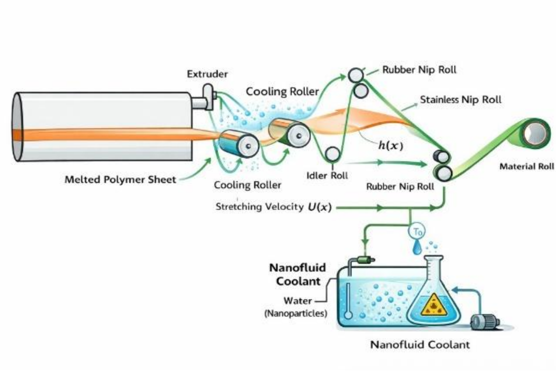

Figure 1: Extrusion model and fluid flow configuration

$$\frac{\partial \tilde{u}}{\partial x} = -\frac{\partial \tilde{v}}{\partial y} \quad (1)$$

$$\tilde{u}\frac{\partial \tilde{u}}{\partial x} + \tilde{v}\frac{\partial \tilde{u}}{\partial y} = \frac{\mu_{nf}}{\rho_{nf}}\frac{\partial^2 \tilde{u}}{\partial y^2} - \frac{\sigma_{nf}}{\rho_{nf}}{B_0}^2\tilde{u} \quad (2)$$

$$\tilde{u}\frac{\partial \tilde{T}}{\partial x} + \tilde{v}\frac{\partial \tilde{T}}{\partial y} = \frac{k_{nf}}{(\rho c_p)_{nf}}\frac{\partial^2 \tilde{T}}{\partial y^2} - \lambda_T\left(\tilde{u}^2\frac{\partial^2 \tilde{T}}{\partial x^2} + \tilde{v}^2\frac{\partial^2 \tilde{T}}{\partial x^2} + 2\tilde{u}\tilde{v}\frac{\partial^2 \tilde{T}}{\partial x \partial y} + \tilde{u}\frac{\partial \tilde{u}}{\partial x}\frac{\partial \tilde{T}}{\partial x} + \tilde{u}\frac{\partial \tilde{v}}{\partial x}\frac{\partial \tilde{T}}{\partial y} + \tilde{v}\frac{\partial \tilde{u}}{\partial y}\frac{\partial \tilde{T}}{\partial x} + \tilde{v}\frac{\partial \tilde{v}}{\partial y}\frac{\partial \tilde{T}}{\partial y}\right) \quad (3)$$

2.1. Boundary conditions.

$$\tilde{u} = u_w(x) = A_0(x+b)^m,\ \tilde{T} = T_w(x),\ \tilde{v} = 0 \quad \text{at} \quad y = A_1(x+b)^{\frac{1-m}{2}}$$

$$\tilde{u} \to 0,\ \tilde{T} \to T_\infty \quad \text{as } y \to \infty \quad (4)$$

with velocity components in the x and y directions as $\tilde{u}$ and $\tilde{v}$ respectively. λ_T is the thermal relaxation time, μ_{nf} denotes dynamic viscosity, k_{nf} is thermal conductivity of nanofluid, ρ_{nf} is density of nanofluid and $(cp)_{nf}$ denotes nanofluid heat capacity. Let us introduce a similarity variable ξ to reduce multivariable differential equations ibn terms of single variable ξ

$$\tilde{u} = A_0(x+b)^m F'(\xi), \qquad \tilde{v} = -\sqrt{\frac{(m+1)}{2}\nu_f A_0}(x+b)^{\frac{m-1}{2}}\left(F(\xi) + \xi F'(\xi)\frac{m-1}{m+1}\right)$$

$$\psi(\xi) = F(\xi)\sqrt{\frac{2}{m+1}\nu_f A_0}(x+b)^{\frac{m+1}{2}},\ \Theta(\xi) = \frac{\tilde{T}-\tilde{T}_\infty}{\tilde{T}_w-\tilde{T}_\infty}, \xi = y\sqrt{\frac{(m+1)}{2\nu_f}A_0}(x+b)^{\frac{m-1}{2}} \quad (5)$$

Hence by stream function, the velocity terms can be expressed as $\tilde{u} = \frac{\partial \psi}{\partial y}$ and $\tilde{v} = -\frac{\partial \psi}{\partial x}$. Using the similarity transformations (5) in equations (2) ,(3)and (4),

$$F''' + \frac{A_2}{A_1}\left(FF'' - \frac{2m}{m+1}F'^2\right) - \frac{A_5}{A_1}M\left(\frac{2}{m+1}\right)F' = 0 \quad (6)$$

$$\Theta'' + Pr\frac{A_3}{A_4}F\Theta' + \gamma Pr\frac{A_3}{A_4}\left(\frac{m-3}{2}FF'\Theta' - \frac{m+1}{2}F^2\Theta''\right) = 0 \quad (7)$$

and boundary conditions can be written as

$$F(\alpha) = \alpha\left(\frac{1-m}{1+m}\right), F'(\alpha) = 1, \Theta(\alpha) = 1, F'(\infty) = 0, \Theta(\infty) = 0 \quad (8)$$

The parameter $\alpha = A_1\sqrt{\frac{m+1}{2\nu_f}A_0}$ is defined as the wall thickness.

Setting $\eta = \xi - \alpha, F(\xi) = F(\xi-\alpha) = f(\eta)$ and $\Theta(\xi) = \Theta(\xi-\alpha) = \theta(\eta)$. The equations (6)-(8) becomes

$$f''' + \frac{A_2}{A_1}\left(ff'' - \frac{2m}{m+1}f'^2\right) - \frac{A_5}{A_1}M\left(\frac{2}{m+1}\right)f' = 0 \quad (9)$$

$$\theta'' + Pr\frac{A_3}{A_4}f\theta' + \gamma Pr\frac{A_3}{A_4}\left(\frac{m-3}{2}ff'\theta' - \frac{m+1}{2}f^2\theta''\right) = 0 \quad (10)$$

With the following boundary conditions,

$$f(\eta) = \alpha\left(\frac{1-m}{1+m}\right), \frac{\partial f}{\partial \eta} = 1, \theta(\eta) = 1 \text{ at } \eta = 0$$

$$\frac{\partial \theta}{\partial \eta} = 0, \theta = 0 \quad \text{at} \quad \eta = \infty \quad (11)$$

here m is power index of velocity,M is magnetic parameter, wall thickness parameter α, Prandtl number Pr and Thermal relaxation time γ, are the non-dimensional parameters that appear in equations (12)-(14). These parameters are defined as

$$M = \frac{\sigma_f {B_0}^2(x+b)}{\rho_f u_w}, \alpha = A_1\sqrt{\frac{m+1}{2\nu_f}A_0}, Pr = \frac{\nu_f(\rho c_p)_f}{k_f}, \gamma = \lambda_T A_0(x+b)^{m-1}$$

The expression for A_1, A_2, A_3, A_4 & A_5 appearing in equations (9)-(11) due to the nanofluid is given as $A_1 = \frac{\mu_{nf}}{\mu_f}$, $A_2 = \frac{\rho_{nf}}{\rho_f}$, $A_3 = \frac{(\rho C_p)_{nf}}{(\rho C_p)_f}$, $A_4 = \frac{k_{nf}}{k_f}$, $A_5 = \frac{\sigma_{nf}}{\sigma_f}$,

Xue thermal conductivity model [52]

$$\frac{k_{nf}}{k_f} = \frac{1-\phi-2\phi\left(\frac{k_{np}}{k_f-k_{np}}\right)\ln\left(\frac{k_f+k_{np}}{2k_f}\right)}{1-\phi-2\phi\left(\frac{k_f}{k_f-k_{np}}\right)\ln\left(\frac{k_f+k_{np}}{2k_f}\right)} \quad (12)$$

Yamada-Ota thermal conductivity model [52]

$$\frac{k_{nf}}{k_f} = \frac{\frac{k_{np}}{k_f}+2\phi^{0.2}\frac{L}{R}-2\phi\phi^{0.2}\frac{L}{R}\left(1-\frac{k_{np}}{k_f}\right)}{\frac{k_{np}}{k_f}+2\phi^{0.2}\frac{L}{R}+\phi\left(1-\frac{k_{np}}{k_f}\right)} \quad (13)$$

Here, K denotes the shape factor, which for cylindrical particles is given by the expression $K = 2\phi^{0.2}\frac{L}{D}$. where L and D represent the length and diameter of the cylindrical particles, respectively. According to the measurements reported in [53], the average length and diameter of the carbon nanotubes (CNTs) are approximately 10 μm and 150 nm. The subscripts f, nf and np denote base fluid, nanofluid and nanoparticle respectively. Thermo-physical properties of water and nanoparticle is listed in Table 1.

Table 1: Thermo-physical properties of water and nanoparticle [53]

Thermo-physical properties	ρ(kg /m^3)	C_p(J /kg K)	k(W /m K)	σ(S /m)
Water	997.1	4179	0.613	0.05
CNT	2600	425	6600	0.5×10^{-6}

The skin friction coefficient(C_{fx}) at the surface and the Nusselt number (Nu_x) are $C_{fx} = \frac{\tau_w}{\rho_f {u_w}^2}$, $Nu_x = \frac{(x+b)\theta_w}{k_f(T_w-T_\infty)}$ after simplification of shear stress and heat flux terms and using similarity variable the non-dimensional form of these two physical quantities can be written as: $\sqrt{Re_x}C_{fx} = A_1\sqrt{\frac{m+1}{2}}f''(0)$ (14)

$$Nu_x {Re_x}^{-1/2} = -A_4\sqrt{\frac{m+1}{2}}\theta'(0) \quad (15)$$

where $Re_x = \frac{(x+b)U_w}{\upsilon}$ is local Reynold's Number.

3. Results and discussion.

In this research article, the authors investigated the effects of various parameters, including the magnetic parameter, on the system under consideration. (M), volume fraction of nanoparticle (ϕ), wall thickness parameter (α) and thermal relaxation parameter(γ) on dimensionless profiles $f'(\eta), \theta(\eta)$ and $Nu_x {Re_x}^{-1/2}$ is scrutinized through graphical representations. Except in plotting of graph, the values of influencing parameters are fixed as $M = 1, \phi = 0.02, \alpha = 0.1, \gamma = 0.1, Pr = 6.8$. The influence of the magnetic parameter (M) upon velocity is depicted in figures 2a & 2b. The magnetic parameter (M) represents the effect of a magnetic field on an electrically conducting fluid. From Figures 2a and 2b .It is noticed that magnetic parameter accelerates the momentum profile and also energy profile is diminished for higher values of magnetic parameter. Increasing the magnetic parameter (M) reduces the velocity and causes the fluid to diverge as it moves along the surface. The influence of the magnetic parameter in reducing velocity is more pronounced due to the spreading of the flow. When a magnetic field is applied, it induces a resistive force called the Lorentz force. This force opposes the motion of the fluid, thereby reducing the velocity even further.The influence of magnetic parameter on the temperature distribution under varying magnetic field strengths is depicted in Figures 3a and 3b. Increase in the magnetic parameter results in a reduction in velocity near the surface. This decrease thickens the thermal boundary layer and raises the surface temperature due to diminished convective heat transfer.

Figures 4a and 4b depict how varying the nanoparticle volume fraction affects the velocity distribution. As the volume fraction increases, the fluid velocity decreases, primarily due to heightened viscosity and increased resistance to flow. This contrasting behaviour is more prominently captured by the Yamada–Ota model, which more effectively accounts for nanoparticle interaction effects compared to the Xue model.

Figures 5a and 5b show the effects of nanoparticle volume fraction on the thermal profile. Increased nanoparticle concentration enhances thermal conductivity, leading to elevated temperatures near the surface and a thickened thermal boundary layer. However, convex sheets exhibit more substantial temperature rises due to higher flow separation and drag. Concave sheets, maintaining better flow attachment, experience a comparatively moderate increase in temperature. Again, the Yamada–Ota model demonstrates a more significant sensitivity to these changes than the Xue model.

Figures 6a and 6b present the impact of the wall thickness parameter α on the velocity profile. For $m < 1$, increasing α decreases the stretching velocity, thereby reducing the flow velocity. For $m > 1$, while the stretching velocity increases with α, the added thickness may still introduce resistance near the surface, moderating the overall flow velocity. In both cases, a thicker wall tends to reduce the boundary layer thickness, thus altering the velocity distribution

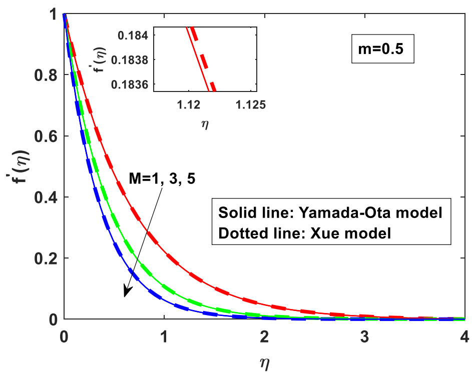

Figure 2a: Impact magnetic parameter on velocity for m = 0.5.

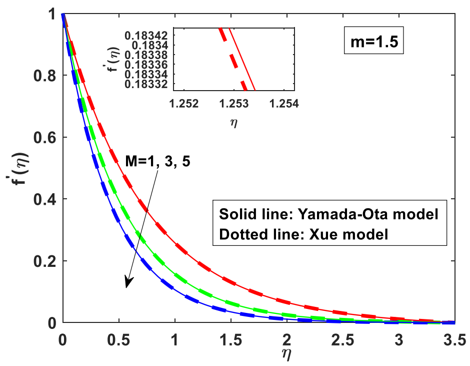

Figure 2b: Impact magnetic parameter on velocity for m = 1.5.

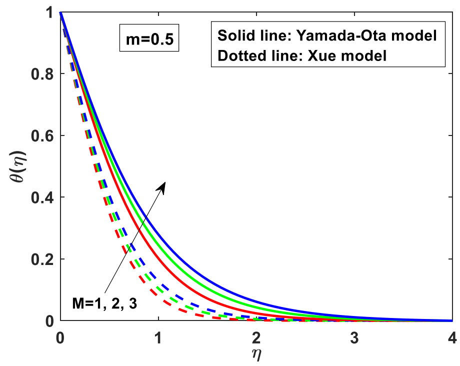

Figure 3a: Impact energy profile for m = 0.5.

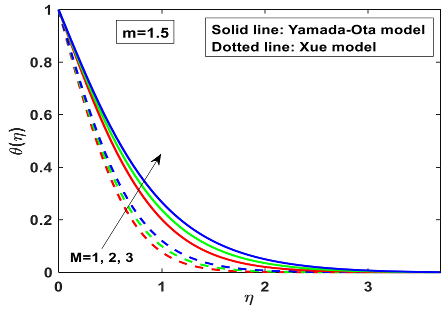

Figure 3b: Impact energy profile for m = 0.5.

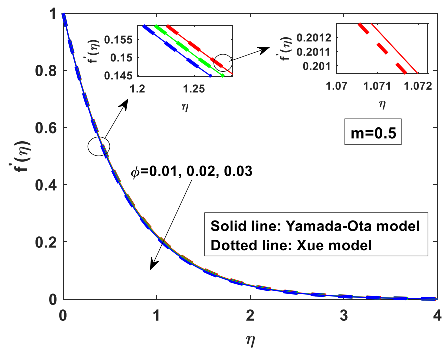

Figure 4a: Impact of nanoparticle volume fraction on velocity for m = 0.5.

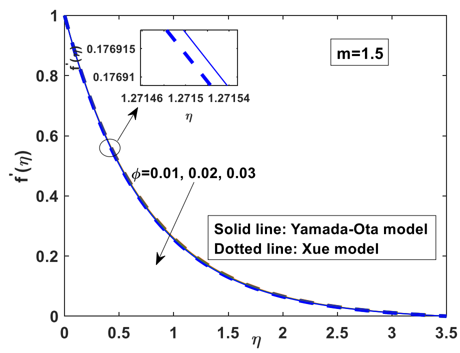

Figure 4b: Impact of nanoparticle volume fraction on velocity for m = 1.5.

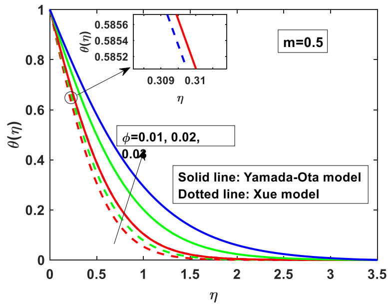

Figure 5a: Impact of nanoparticle volume fraction on temperature for m = 0.5.

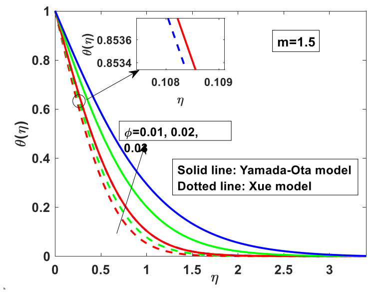

Figure 5b: Impact of nanoparticle volume fraction on temperature for m = 1.5.

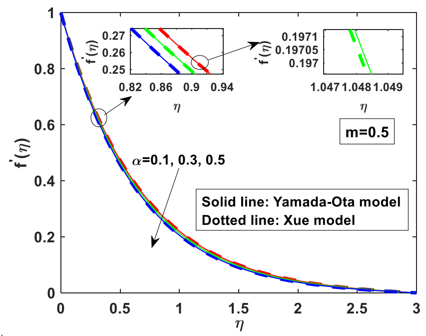

Figure 6a: Impact of wall thickness parameter on velocity for m = 0.5.

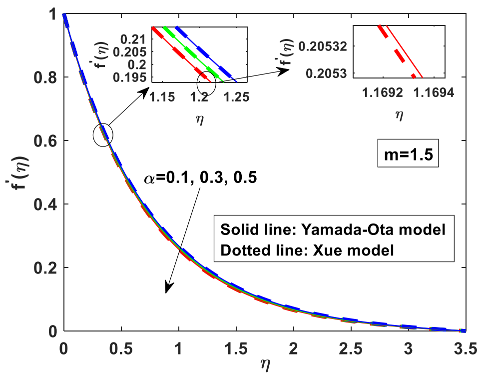

Figure 6b: Impact of wall thickness parameter on velocity for m = 1.5.

4. Concluding remarks.

The study investigates the influence of several parameters—magnetic field strength (M), nanoparticle volume fraction (ϕ), wall thickness (α), and thermal relaxation parameter (γ)—on the velocity and temperature profiles, as well as the Nusselt number in nanofluid systems. The effects are analysed for different sheet geometries, including convex (m < 1), concave (m > 1) sheets, using both the Xue and Yamada-Ota models.

- The temperature increases near the sheet with increasing M due to a thicker thermal boundary layer caused by reduced velocity.
- A higher value of wall thickness parameter α results in decreased velocity due to increased drag and flow separation.
- Temperature increases with thicker walls due to reduced convective heat transfer, with convex sheets showing a more pronounced rise in surface temperature.
- The Yamada-Ota model provides higher and more accurate predictions for heat transfer than the Xue model, particularly due to its better representation of CNT nanofluid properties.

References

[1] Y. Xuan and Q. Li, "Heat transfer enhancement of nanofluids," *Int. J. Heat Fluid Flow*, vol. 21, no. 1, pp. 58–64, 2000, doi: 10.1016/S0142-727X(99)00067-3.

[2] N. Sandeep, B. Rushi Kumar, and M. S. Jagadeesh Kumar, "A comparative study of convective heat and mass transfer in non-Newtonian nanofluid flow past a permeable stretching sheet," *J. Mol. Liq.*, vol. 212, pp. 585–591, 2015, doi: 10.1016/j.molliq.2015.10.010.

[3] C. S. K. Raju, N. Sandeep, and A. Malvandi, "Free convective heat and mass transfer of MHD non-Newtonian nanofluids over a cone in the presence of non-uniform heat source/sink," *J. Mol. Liq.*, vol. 221, pp. 108–115, 2016, doi: 10.1016/j.molliq.2016.05.078.

[4] M. Z. A. Qureshi, Q. Rubbab, S. Irshad, S. Ahmad, and M. Aqeel, "Heat and Mass Transfer Analysis of MHD Nanofluid Flow with Radiative Heat Effects in the Presence of Spherical Au-Metallic Nanoparticles,"

Nanoscale Res. Lett., vol. 11, no. 1, 2016, doi: 10.1186/s11671-016-1692-2.

[5] J. V. Ramana Reddy, V. Sugunamma, and N. Sandeep, "Enhanced heat transfer in the flow of dissipative non-Newtonian Casson fluid flow over a convectively heated upper surface of a paraboloid of revolution," *J. Mol. Liq.*, vol. 229, pp. 380–388, 2017, doi: 10.1016/j.molliq.2016.12.100.

[6] M. N. Rostami, S. Dinarvand, and I. Pop, "Dual solutions for mixed convective stagnation-point flow of an aqueous silica–alumina hybrid nanofluid," *Chinese J. Phys.*, vol. 56, no. 5, pp. 2465–2478, 2018, doi: 10.1016/j.cjph.2018.06.013.

[7] I. Khan, K. Saeed, and I. Khan, "Nanoparticles: Properties, applications and toxicities," *Arab. J. Chem.*, vol. 12, no. 7, pp. 908–931, 2019, doi: 10.1016/j.arabjc.2017.05.011.

[8] I. Rashid, M. Sagheer, and S. Hussain, "Entropy formation analysis of MHD boundary layer flow of nanofluid over a porous shrinking wall," *Phys. A Stat. Mech. its Appl.*, vol. 536, 2019, doi: 10.1016/j.physa.2019.122608.

[9] I. Waini, A. Ishak, and I. Pop, "Hybrid nanofluid flow induced by an exponentially shrinking sheet," *Chinese J. Phys.*, vol. 68, pp. 468–482, 2020, doi: 10.1016/j.cjph.2019.12.015.

[10] J. V. Ramana Reddy, V. Sugunamma, and N. Sandeep, "Impact of nonlinear radiation on 3D magnetohydrodynamic flow of methanol and kerosene based ferrofluids with temperature dependent viscosity," *J. Mol. Liq.*, vol. 236, pp. 93–100, 2017, doi: 10.1016/j.molliq.2017.04.011.

[11] R. J. Punith Gowda, R. Naveen Kumar, B. C. Prasannakumara, B. Nagaraja, and B. J. Gireesha, "Exploring magnetic dipole contribution on ferromagnetic nanofluid flow over a stretching sheet: An application of Stefan blowing," *J. Mol. Liq.*, vol. 335, p. 116215, 2021, doi: 10.1016/j.molliq.2021.116215.

[12] N. Vishnu Ganesh, A. J. Chamkha, Q. M. Al-Mdallal, and P. K. Kameswaran, "Magneto-Marangoni nano-boundary layer flow of water and ethylene glycol based γ Al2O3 nanofluids with non-linear thermal radiation effects," *Case Stud. Therm. Eng.*, vol. 12, pp. 340–348, 2018, doi: 10.1016/j.csite.2018.04.019.

[13] P. K. Dadheech, P. Agrawal, A. Sharma, K. S. Nisar, and S. D. Purohit, "Marangoni convection flow of γ–Al2O3 nanofluids past a porous stretching surface with thermal radiation effect in the presence of an inclined magnetic field," *Heat Transf.*, vol. 51, no. 1, pp. 534–550, 2022, doi: 10.1002/htj.22318.

[14] Y. Lin, B. Li, L. Zheng, and G. Chen, "Particle shape and radiation effects on Marangoni boundary layer flow and heat transfer of copper-water nanofluid driven by an exponential temperature," *Powder Technol.*, vol. 301, pp. 379–386, 2016, doi: 10.1016/j.powtec.2016.06.029.

[15] T. Hayat, M. I. Khan, M. Farooq, A. Alsaedi, and T. Yasmeen, "Impact of Marangoni convection in the flow of carbon–water nanofluid with thermal radiation," *Int. J. Heat Mass Transf.*, vol. 106, pp. 810–815, 2017, doi: 10.1016/j.ijheatmasstransfer.2016.08.115.

[16] D. M. Christopher and B. Wang, "Prandtl number effects for Marangoni convection over a flat surface," *Int. J. Therm. Sci.*, vol. 40, no. 6, pp. 564–570, 2001, doi: 10.1016/S1290-0729(01)01244-3.

[17] A. J. Chamkha, I. Pop, and H. S. Takhar, "Marangoni mixed convection boundary layer flow," *Meccanica*, vol. 41, no. 2, pp. 219–232, 2006, doi: 10.1007/s11012-005-3352-y.

[18] Q. M. Al-Mdallal, N. Indumathi, B. Ganga, and A. K. Abdul Hakeem, "Marangoni radiative effects of hybrid-nanofluids flow past a permeable surface with inclined magnetic field," *Case Stud. Therm. Eng.*, vol. 17, no. December 2019, p. 100571, 2020, doi: 10.1016/j.csite.2019.100571.

[19] E. Magyari and A. J. Chamkha, "Exact analytical solutions for thermosolutal

Marangoni convection in the presence of heat and mass generation or consumption," *Heat Mass Transf. und Stoffuebertragung*, vol. 43, no. 9, pp. 965–974, 2007, doi: 10.1007/s00231-006-0171-1.

[20] L. Zheng, X. Zhang, and Y. Gao, "Analytical solution for Marangoni convection over a liquid-vapor surface due to an imposed temperature gradient," *Math. Comput. Model.*, vol. 48, no. 11–12, pp. 1787–1795, 2008, doi: 10.1016/j.mcm.2008.04.003.

[21] E. H. Aly and A. Ebaid, "Exact analysis for the effect of heat transfer on MHD and radiation Marangoni boundary layer nanofluid flow past a surface embedded in a porous medium," *J. Mol. Liq.*, vol. 215, pp. 625–639, 2016, doi: 10.1016/j.molliq.2015.12.108.

[22] B. Mahanthesh, B. J. Gireesha, N. S. Shashikumar, and S. A. Shehzad, "Marangoni convective MHD flow of SWCNT and MWCNT nanoliquids due to a disk with solar radiation and irregular heat source," *Phys. E Low-Dimensional Syst. Nanostructures*, vol. 94, pp. 25–30, 2017, doi: 10.1016/j.physe.2017.07.011.

[23] N. Ahmed, Adnan, U. Khan, and S. T. Mohyud-Din, "Influence of an effective Prandtl number model on squeezed flow of γAl2O3-H2O and γAl2O3-C2H6O2 nanofluids," *J. Mol. Liq.*, vol. 238, pp. 447–454, 2017, doi: 10.1016/j.molliq.2017.05.049.

[24] B. Mahanthesh and B. J. Gireesha, "Scrutinization of thermal radiation, viscous dissipation and Joule heating effects on Marangoni convective two-phase flow of Casson fluid with fluid-particle suspension," *Results Phys.*, vol. 8, pp. 869–878, 2018, doi: 10.1016/j.rinp.2018.01.023.

[25] T. S. Wang and W. Y. Shi, "Influence of substrate temperature on Marangoni convection instabilities in a sessile droplet evaporating at constant contact line mode," *Int. J. Heat Mass Transf.*, vol. 131, pp. 1270–1278, 2019, doi: 10.1016/j.ijheatmasstransfer.2018.11.155.

[26] Y. J. Zhuang and Q. Y. Zhu, "Numerical study on combined buoyancy–Marangoni convection heat and mass transfer of power-law nanofluids in a cubic cavity filled with a heterogeneous porous medium," *Int. J. Heat Fluid Flow*, vol. 71, no. July 2017, pp. 39–54, 2018, doi: 10.1016/j.ijheatfluidflow.2018.03.006.

[27] S. Mukhopadhyay and G. C. Layek, "Effects of thermal radiation and variable fluid viscosity on free convective flow and heat transfer past a porous stretching surface," vol. 51, pp. 2167–2178, 2008, doi: 10.1016/j.ijheatmasstransfer.2007.11.038.

[28] K. Khanafer and K. Vafai, "Applications of nanofluids in porous medium A critical review," *J. Therm. Anal. Calorim.*, vol. 4, 2018, doi: 10.1007/s10973-018-7565-4.

[29] P. K. Dadheech, P. Agrawal, S. D. Purohit, and D. Kumar, "Study of Flow and Heat Transfer of CuO - Ag / C H O Hybrid Nanofluid over a Stretching Surface with Porous Media and MHD Effect," no. December, pp. 1–8, 2021, doi: 10.14456/scitechasia.2021.78.

[30] N. V. Ganesh, Q. M. Al-Mdallal, S. Al Fahel, and S. Dadoa, "Riga – Plate flow of γ Al 2 O 3 -water/ethylene glycol with effective Prandtl number impacts," *Heliyon*, vol. 5, no. 5, p. e01651, 2019, doi: 10.1016/j.heliyon.2019.e01651.

[31] F. Saba, N. Ahmed, U. Khan, and S. T. Mohyud-Din, "Impact of an effective Prandtl number model and across mass transport phenomenon on the γAI2O3 nanofluid flow inside a channel," *Phys. A Stat. Mech. its Appl.*, vol. 526, p. 121083, 2019, doi: 10.1016/j.physa.2019.121083.

[32] M. M. Rashidi, N. Vishnu Ganesh, A. K. Abdul Hakeem, B. Ganga, and G. Lorenzini, "Influences of an effective Prandtl number model on nano boundary layer flow of γ Al2O3-H2O and γ Al2O3-C2H6O2 over a vertical stretching sheet," *Int. J. Heat Mass Transf.*, vol. 98, pp. 616–623, 2016, doi: 10.1016/j.ijheatmasstransfer.2016.03.006.

[33] T. Gul, S. Nasir, S. Islam, Z. Shah, and M. A. Khan, "Effective Prandtl Number Model

Influences on the γAl 2O 3 – H 2O and γAl 2O 3 – C 2H 6O 2 Nanofluids Spray Along a Stretching Cylinder," *Arab. J. Sci. Eng.*, vol. 44, no. 2, pp. 1601–1616, 2019, doi: 10.1007/s13369-018-3626-z.

[34] A. Manuscript, "Ac ce velocity , micro rotation and temperature distribution as well as the skin friction and the Nusselt d M us pt," 2019.

[35] N. V. Ganesh, Q. M. Al-Mdallal, and P. K. Kameswaran, "Numerical study of MHD effective Prandtl number boundary layer flow of γ Al 2 O 3 nanofluids past a melting surface," *Case Stud. Therm. Eng.*, vol. 13, no. February, p. 100413, 2019, doi: 10.1016/j.csite.2019.100413.

[36] S. Qayyum, "Dynamics of Marangoni convection in hybrid nanofluid flow submerged in ethylene glycol and water base fluids," *Int. Commun. Heat Mass Transf.*, vol. 119, p. 104962, 2020, doi: 10.1016/j.icheatmasstransfer.2020.104962.